

## PERFORMANCE-BASED CONNECTION TOPOLOGY OPTIMIZATION OF UNBRACED AND X-BRACED STEEL FRAMES

H. Rahami<sup>1\*</sup>, P. Mohebian<sup>2</sup> and M. Mousavi<sup>2</sup>

<sup>1</sup>*School of Engineering Science, College of Engineering, University of Tehran, Tehran, Iran*

<sup>2</sup>*Department of Civil Engineering, Faculty of Engineering, Arak University, Iran*

### ABSTRACT

The present study sets out to integrate the performance-based seismic design approach with the connection topology optimization method. Performance-based connection topology optimization concept aims to simultaneously optimize the size of members and the type of connections with respect to the framework of performance-based seismic design. This new optimization concept is carried out for unbraced and X-braced steel frames in order to assess its efficiency. The cross-sectional area of components and the type of beam-to-column connections are regarded as design variables. The objective function is formulated in terms of the material costs and the cost of rigid connections. The nonlinear pushover analysis is adopted to acquire the response of the structure at various performance levels. In order to cope with the optimization problem, CBO algorithm is employed. The achieved results demonstrate that incorporating the optimal arrangement of beam-to-column connections into the optimum performance-based design procedure of either unbraced or X-braced steel frame could lead to a design that significantly reduces the overall cost of the structure and offers a predictable and reliable performance for the structure subjected to hazard levels.

**Keywords:** performance-based seismic design; connection topology optimization; colliding bodies optimization algorithm; steel frames; connection arrangement.

Received: 12 November 2016; Accepted: 14 February 2017

### 1. INTRODUCTION

One of the main challenges faced by structural engineers is to achieve a design that is superior in terms of safety and cost effectiveness. The structural optimization approach has

---

\*Corresponding author: School of Engineering Science, College of Engineering, University of Tehran, Tehran, Iran

†E-mail address: hrahami@ut.ac.ir (H. Rahami)

emerged as an efficient means to fulfill this goal. In this way, first, the structural design process is formulated in the framework of an optimization problem, and then an optimization technique is applied to tackle the problem. The ultimate solution of such a mathematical problem not only satisfies the design criteria but also reveals an optimal feature for the structure.

Over the last decades, extensive studies have been accomplished on developing various optimization techniques. Generally, optimization techniques can be classified into traditional gradient-based algorithms and metaheuristic algorithms. Metaheuristic algorithms, which are inspired by natural laws, are more applicable than other category. This can be attributed to the fact that metaheuristic algorithms do not rely on any derivation information about the problem. Furthermore, they are more convenient to implement, and they can also more successfully address the optimization problems. Genetic algorithms (GAs) [1], particle swarm optimization (PSO) [2], and ant colony optimization (ACO) [3] are among the most well-known and widely used metaheuristic techniques. The application of metaheuristic algorithms in the field of structural optimization has received considerable attention in recent years.

In design optimization of steel structures, it is common to simplify the cost optimization problem into the weight optimization problem with respect to the assumption of constant unit cost for each component. Much of the available literature addressing the design optimization of steel frames is concerned with the weight minimization of the structure. Hasançebi et al. [4] applied several metaheuristic algorithms to optimum design of braced and unbraced steel frames subjected to both gravity and lateral loads. The design constraints including axial stress-bending stress interaction, lateral displacement, and geometry restriction, were implemented according to ASD-AISC design code. Dogan and Saka [5] employed particle swarm method to minimize the total weight of unbraced steel frames in accordance with LRFD-AISC specification. Kaveh and Talatahari [6] developed a discrete version of charged system search (CSS) algorithm for the optimum design of some benchmark steel frames and compared the obtained results with those of other methods. Kaveh and Farhoudi [7] adopted GA, ACO, PSO and BB-BC algorithms to perform the layout optimization of dual system of moment frame subjected to serviceability and strength constraints. In addition to linear static analysis approach, structural optimization can be accomplished in the framework of performance-based seismic design (PBSD) by taking advantage of metaheuristic algorithms. PBSD aims to attain a design that possesses more predictable and reliable performance subjected to predefined hazard levels. The performance-based weight optimization of steel structures utilizing metaheuristic algorithms has generated considerable recent research interest. Kaveh et al. [8] applied ACO and GA metaheuristic algorithms for performance-based optimum seismic design of steel frames. In order to obtain the response of the structure at the performance levels a simple computer-based push-over analysis, which is comprised of both the first-order and the second-order geometric properties, was employed. Gholizadeh and Moghadas [9] proposed an improved quantum particle swarm optimization (IQPSO) metaheuristic algorithm for implementation of optimum performance-based seismic design of steel frames subjected to performance constraints on inter-story drift ratio at various performance levels. Talatahari et al. [10] developed a hybrid optimization method based on charged system search algorithm for the performance-based optimum design of steel structures. They also compared their achieved

results with those attained by other algorithms. Gholizadeh and Poorhoseini [11] carried out seismic performance-based layout optimization for steel braced frames by developing an improved dolphin echolocation metaheuristic algorithm. The cross-sections of beams, columns, and braces along with the location of braces in the frame were chosen as design variables.

The simplification that enables the objective function to be formulated in terms of the structural weight is no longer valid if different types of connections are taken into consideration. In this case, the objective function must be representative of the total structural costs. Hayalioglu and Degertekin [12] applied genetic algorithm for minimum cost design of steel frames with semi-rigid connections. The objective function was considered as the sum of the cost of materials and the cost of semi-rigid connections, which relies on the connection rotational stiffness. Hadidi and Rafiee [13] proposed a hybrid algorithm based on combining Harmony Search (HS) and Big Bang-Big Crunch (BB-BC) algorithms for minimum cost design of semi-rigid steel frames subjected to lateral displacement and stress constraints. Kripakaran et al. [14] made a valuable and interesting contribution to develop a framework for minimum cost design of steel moment frames subjected to wind loads by applying a trade-off between the material and connection costs. Each beam-to-column connection was considered to be either simple or rigid. The objective function was specified in terms of material cost and only rigid connection fabrication cost. They used a series of GA algorithm to find the optimal location of a predefined number of rigid joints. Then the results were fed into a heuristic algorithm to optimize the size of elements. It was argued that this strategy helps to achieve a more economic design. Alberdi et al. [15] conducted simultaneous optimization of member sizes and beam-to-column connection types, which was briefly called connection topology optimization, by making use of GA, TS, ACO, and HS metaheuristic algorithms. Their results demonstrated that metaheuristic algorithms are efficient means to perform connection topology optimization. Very Recently, Kaveh et al. [16] accomplished connection topology optimization for seismic design of steel moment frames. They utilized linear static analysis to accomplish this work.

In this paper, performance-based seismic design approach is coupled onto connection topology optimization technique in order to achieve minimum cost design of unbraced and X-braced steel frames. For the present optimization problem, the size of members and the type of connections are considered as design variables. The objective function is formulated with regards to the material cost and rigid connection fabrication cost. The nonlinear pushover analysis is carried out to capture the response of the structure at various performance levels. In order to perform the optimization task, colliding bodies optimization (CBO) [17], which is a robust and parameter-less algorithm, is adopted. In addition to performance-based connection topology optimization, performance-based pure sizing optimization is also carried out for the structures. Then the results attained in these two manners are compared in terms of cost and performance.

## 2. PERFORMANCE BASED SEISMIC DESIGN

The performance-based seismic design (PBSD) procedure can be summarized into three steps. First, a performance objective, which integrates a performance level with a given hazard level, is selected. A performance level is correlated with the maximum extent of damage that can be tolerated by the structure. In this paper, according to ASCE-41 [18], immediate occupancy (IO), life safety (LS), and collapse prevention (CP) performance levels are considered to be satisfied by the structure subjected to hazard levels related to the ground motion with 20%, 10% and 2% possibility of occurrence in 50 years, respectively. In the second step, the seismic demands of the structure are determined in terms of both force and deformation. To perform this task, a nonlinear static pushover analysis is employed. In a pushover analysis, the analytical model of the structure including gravity loads is incrementally pushed subject to a predefined constant lateral load pattern, and the overall capacity of the structure as well as force and deformation demands for the components are monitored during each step. After the execution of the pushover analysis, the seismic demands are taken from the response of the structure at the target displacement i.e. maximum roof displacement experienced by the structure during the seismic event. The target displacement is obtained via a trial and error procedure. The pseudo-code of this procedure can be found in [19]. The estimated target displacement can be obtained by the following expression [18]:

$$\delta_t = C_0 C_1 C_2 S_a \frac{T_e^2}{4\pi^2} g \quad (1)$$

where  $C_0$  is an adjustment factor turning the spectral displacement of a SDOF system to a multi degree of freedom (MDOF) system roof displacement,  $C_1$  is a modification factor that correlates the maximum expected inelastic displacements to the elastic displacements,  $C_2$  stands for the impact of the pinched hysteretic shape on the maximum displacement response,  $T_e$  is the effective fundamental period of the structure, which depends on the elastic fundamental period of the structure obtained by elastic dynamic analysis,  $g$  is the acceleration of gravity, and  $S_a$  is the response spectrum acceleration corresponding to the effective fundamental period and damping ratio of the structure, which is specified as follows [18]:

$$S_a = \begin{cases} S_{XS}^i [(5/B_1 - 2) T/T_S^i + 0.4] & 0 < T < T_0^i \\ S_{XS}^i / B_1 & T_0^i \leq T \leq T_S^i \\ S_{X1}^i / (B_1 T) & T > T_S^i \end{cases}, i = IO, LS, CP \quad (2)$$

where  $S_{XS}^i$  is the design short-period spectral response acceleration parameter,  $S_{X1}^i$  is the design spectral response acceleration at 1-sec period,  $T_0^i$ ,  $T_S^i$ , and  $B_1$  are defined as follows [18]:

$$T_S^i = S_{X1}^i / S_{XS}^i, i = IO, LS, CP \quad (3)$$

$$T_0^i = 0.2 T_S^i, i = IO, LS, CP \quad (4)$$

$$B_1 = 4 / [5.6 - \ln(100\beta)] \quad (5)$$

where  $\beta$  is the effective damping ration which is considered here as 0.05.

In the final step, the structural performance is assessed by comparing the estimated seismic demands against the acceptance criteria. In the present study, the acceptance criteria for the steel frames given by ASCE-41 [18] are adopted for the seismic performance assessment of the frame members.

### 3. STATEMENT OF THE OPTIMIZATION PROBLEM

In the following sub-sections, the formulation characteristics of the present optimization problem are described.

#### 3.1 Design variables

Design variables may appear in the form of topology, geometry, shape, or component properties of the structure [20]. The optimization problem of the present study is mainly composed of two kinds of design variables: sizing design variables (S), including the size of structural members, and connection topology design variables (C), containing the type of each beam-to-column connection as either simple or rigid. Depending on symmetry of the structure and construction considerations, one may assign identical value for a set of design variables to make a design group. The vector of design variables is as follows:

$$X = [S_1, S_2, \dots, S_i, \dots, S_{nS}, C_1, C_2, \dots, C_i, \dots, C_{nC}] \tag{6}$$

where  $i$ ,  $nS$ , and  $nC$  represent the  $i$ th group, the total number of groups for sizing design variables and the total number of groups for connection topology design variables, respectively.

#### 3.2 Objective function

The principal purpose of the present formulation is to seek the best form of the structure including the material distributions and the connection topology in such a way that the total cost of the structure is minimized. According to [14] and [15] the contributions of the material cost as well as rigid connection fabrication cost are taken into account. The cost function of the present optimization problem is as follows:

$$f_{\text{cost}}(X) = \sum_{i=1}^{nc} \rho_i A_i L_i + \frac{C_r}{C_s} \cdot N_R \tag{7}$$

where  $nc$  denotes the total number of components for the structure,  $A_i$  indicates the cross-sectional area for  $i$ th member,  $\rho_j$  and  $L_j$  represent the material mass density and the length of the  $i$ th member,  $N_R$  implies the total number of rigid beam-to-column connections,  $C_s$  is the unit cost of steel material per metric tons and  $C_r$  is the unit cost of the rigid beam-to-column connection. In accordance with [14] and [15] the value for the ratio of  $C_r/C_s$  is taken as 1.5.

### 3.3 Design constraints

In a structural optimization, design constraints provide a means to assess the behavior of the structure based on code requirements. Design constraints can be classified into three types as [21, 11]: serviceability constraints, geometric constraints, and ultimate strength constraints.

#### 3.3.1 Serviceability constraints

At the serviceability stage, the behavior of the structure is evaluated against the gravity loads without the presence of any seismic demands. In this regard, the structural frame is modeled and a gravity load analysis is accomplished under the load combination given by ASCE 7-10 [22]. Then the adequacy of members is recognized according to the LRFD interaction equation of AISC 360-10 [23] as follows:

$$g_{S,i} = \begin{cases} \frac{P_u}{\phi_c P_n} + \frac{8}{9} \left( \frac{M_{ux}}{\phi_b M_{nx}} + \frac{M_{uy}}{\phi_b M_{ny}} \right) \leq 0 & \text{if } \frac{P_u}{\phi_c P_n} \geq 0.2 \\ \frac{P_u}{2\phi_c P_n} + \left( \frac{M_{ux}}{\phi_b M_{nx}} + \frac{M_{uy}}{\phi_b M_{ny}} \right) \leq 0 & \text{if } \frac{P_u}{\phi_c P_n} < 0.2 \end{cases}, i = 1, \dots, nm \quad (8)$$

where  $nm$  represents the total number of frame members (beams and columns),  $P_u$  is the required axial strength,  $M_u$  is the required moment strength,  $P_n$  is the nominal compressive strength,  $M_{nx}$  is nominal moment strength about the strong-axis,  $M_{ny}$  is nominal moment strength about the weak-axis,  $\phi_c$  is the resistance factor for compression and  $\phi_b$  is the resistance factor for bending.

#### 3.3.2 Geometric constraints

For the beam-to-column connection, the flange width of the beam ( $b_f^b$ ) should not be larger than the flange width of the column ( $b_f^c$ ). This type of constraint can be stated as follows [15]:

$$g_{G,i} = \frac{b_f^b}{b_f^c} - 1.0 \leq 0, i = 1, \dots, nbc \quad (9)$$

where  $nbc$  is the number of beam-to-column connections.

#### 3.3.3 Ultimate strength constraints

In PBSO approach, performance of the structure subjected to a given hazard level is measured with respect to strength and deformation of individual components. Deformations, which can be expressed in terms of story drift, are typically utilized to illustrate the overall structural response associated with various performance levels [18].

For unbraced steel frames, structural performance assessment can be carried out by applying inter-story drift constraint at various performance levels as follows [8-11]:

$$g_{d,ub,i}^j = \frac{\delta_{ub,i}^j}{\delta_{ub,all,i}^j} - 1 \leq 0 \quad , i = 1, 2, \dots, ns \quad \& \quad j = IO, LS, CP \quad (10)$$

where  $\delta_{ub,i}^j$  indicates  $i$ th inter-story drift of unbraced steel frame at the  $j$ th performance level, and  $\delta_{ub,all,i}^j$  is the maximum allowable inter-story drift for the unbraced steel frame. As can be found in ASCE-41 [18], the allowable values of inter-story drifts at the IO, LS and CP performance levels are 0.7%, 2.5% and 5.0%, respectively.

For X-braced steel frames, structural performance assessment can be performed by imposing constraints on inter-story drift, plastic hinge rotation of frame members, and axial deformation of braces at the performance levels [11].

The constraint attributed to the inter-story drift for X-braced steel frame at various performance levels can be specified as follows:

$$g_{d,xb,i}^j = \frac{\delta_{xb,i}^j}{\delta_{xb,all,i}^j} - 1 \leq 0 \quad , i = 1, 2, \dots, ns \quad \& \quad j = IO, LS, CP \quad (11)$$

where  $\delta_{xb,i}^j$  represents  $i$ th inter-story drift for X-braced steel frame regarding to the  $j$ th performance level, and  $\delta_{xb,all,i}^j$  is the maximum allowable inter-story drift for the X-braced steel frame. According to ASCE-41 [18], the allowable values of inter-story drifts at the IO, LS and CP performance levels are 0.5%, 1.5% and 2.0%, respectively.

The constraint related to the plastic hinge rotation of frame members at various performance levels can be expressed as follows:

$$g_{r,xb,i}^j = \frac{\theta_{xb,i}^j}{\theta_{xb,all,i}^j} - 1 \leq 0 \quad , i = 1, 2, \dots, nm \quad \& \quad j = IO, LS, CP \quad (12)$$

where  $\theta_{xb,i}^j$  is the value of plastic hinge rotation at each end of  $i$ th member of X-braced steel frame regarding to the  $j$ th performance level, and  $\theta_{xb,all,i}^j$  is the allowable plastic hinge rotation of  $i$ th frame member for the performance level  $j$ . In accordance with ASCE-41 [18], the allowable values of plastic hinge rotation at the IO, LS and CP performance levels are  $\theta_y$ ,  $6\theta_y$  and  $8\theta_y$ , respectively.  $\theta_y$  is the rotation at yield, which can be obtained as follows [18]:

$$\theta_y = \begin{cases} \frac{ZF_{ye}L_b}{6EI_b}, & \text{Bams} \\ \frac{ZF_{ye}L_c}{6EI_c} \left(1 - \frac{P}{P_{ye}}\right), & \text{Columns} \end{cases} \quad (13)$$

in which  $Z$  is plastic section modulus,  $F_{ye}$  is the expected yield strength of material,  $L_b$  is the length of beam,  $L_c$  is the length of column,  $E$  is the modulus of elasticity,  $I$  represents

moment of inertia,  $P$  denotes the axial force in the member at the target displacement,  $P_{ye}$  is the expected axial yield force of member.

The constraint associated with axial deformation of braces at various performance levels can be stated as follows:

$$g_{d,xb,i}^j = \frac{\Delta_i^j}{\Delta_{all,i}^j} - 1 \leq 0 \quad , i = 1, 2, \dots, nb \quad \& \quad j = IO, LS, CP \quad (14)$$

where  $nb$  is the total number of braces,  $\Delta_i^j$  denotes the axial deformation of  $i$ th brace regarding to the  $j$ th performance level, and  $\Delta_{all,i}^j$  is the maximum allowable axial deformation for braces. In line with ASCE-41 [18],  $\Delta_{all,i}^j$  for braces in tension at the IO, LS and CP performance levels are  $0.25\Delta_T$ ,  $7\Delta_T$  and  $9\Delta_T$ , respectively, in which  $\Delta_T$  is the axial deformation at expected tensile yielding load. Furthermore,  $\Delta_{all,i}^j$  for braces in compression at the LS and CP performance levels are  $0.25\Delta_C$ ,  $5\Delta_C$  and  $7\Delta_C$ , respectively, in which  $\Delta_C$  is the axial deformation at expected buckling load.

### 3.4 Constraint handling approach

In this study, a penalty function method is applied to deal with such a constrained optimization problem. This approach converts the constrained optimization problem into an unconstrained one as follows [24]:

$$Z(X) = f_{cost}(X) \times f_{penalty}(X) = f_{cost}(X) \times \left( 1 + \varepsilon_1 \cdot \sum_{i=1}^q \max(0, g_i(X)) \right)^{\varepsilon_2} \quad (15)$$

where  $Z(X)$  represents the penalized objective function,  $f_{penalty}(X)$  is the penalty function,  $g_i(X)$  is the  $i$ th constraint,  $q$  is the total number of constraints  $\varepsilon_1$  and  $\varepsilon_2$  are two parameters selected based on the exploration and the exploitation rate of the design space. According to [25]  $\varepsilon_1$  is taken as unit, and  $\varepsilon_2$  is obtained at each iteration ( $iter$ ) as follows:

$$\varepsilon_2 = 1.5 + 1.5 \times \frac{iter}{iter_{max}} \quad (16)$$

In which  $iter_{max}$  is the maximum number of iterations specified for the optimization algorithm.

## 4. OPTIMIZATION ALGORITHM

The CBO metaheuristic algorithm, which has been developed by Kaveh and Mahdavi [17], benefits from the collision and momentum conservation principle. This method, as a population-based algorithm, contains a number of agents, known as colliding bodies. The



position of each colliding body in the search space indicates decision variables of its corresponding candidate solution. Also, the mass of each colliding body is in relation to the value of individual objective function, which is normalized by the total mass of agents. For a minimization problem, the mass of each colliding body can be measured as follows [17]:

$$m_i = \frac{1/\text{fit}_i}{\sum_{l=1}^n 1/\text{fit}_l} \tag{17}$$

where *fit* represents the objective function value of the solution, and *n* is the size of population.

The CBs are sorted in an ascending sequence in accordance with their fitness function values. After that, the agents are divided into two groups of equal size. The collision is considered that occurs between the corresponding members of the stationary and moving groups. Moreover, it is assumed that the physical contact between each two colliding bodies is taken place at the position of the better particle. Therefore, the first group, which is comprised of better agents, is called stationary group, and the other, which comes close to the first group is called moving group. Under these conditions, the velocities of the stationary and moving objects before the collision can be stated as follows [17]:

$$v_i = 0, \quad i = 1, 2, \dots, \frac{n}{2} \tag{18}$$

$$v_i = x_{i-\frac{n}{2}} - x_j, \quad i = \frac{n}{2} + 1, \frac{n}{2} + 2, \dots, n \tag{19}$$

where  $v_i$  is the velocity vector of *i*th CB.

The collision between two objects gives rise to a changes in their velocities. The velocity of each stationary and moving CBs after the collision ( $v'_i$ ) is defined by [17]:

$$v'_i = \frac{(m_{i+\frac{n}{2}} + \epsilon m_{i+\frac{n}{2}})v_{i+\frac{n}{2}}}{m_i + m_{i+\frac{n}{2}}}, \quad i = 1, 2, \dots, \frac{n}{2} \tag{20}$$

$$v'_i = \frac{(m_i - \epsilon m_{i-\frac{n}{2}})v_i}{m_i + m_{i-\frac{n}{2}}}, \quad i = 1 + \frac{n}{2}, \frac{n}{2} + 2, \dots, n \tag{21}$$

where  $\epsilon$  is the coefficient of restitution (COR), which is devised as a means to adjust the rates of the exploration and the exploitation in the optimization process. The value of this parameter declines linearly from unit to zero with respect to the ratio of the current iteration number (*iter*) to the maximum number of iteration (*iter<sub>max</sub>*) for the optimization procedure as follows [17]:

$$\epsilon = 1 - \frac{\text{iter}}{\text{iter}_{\max}} \tag{22}$$

Considering the fact that the velocities of CBs correlate with their displacements, the

new positions of the stationary and moving bodies can be obtained with regards to their new velocities at the position of the stationary bodies as follows [17]:

$$x_i^{new} = x_i + rand \circ v'_i, \quad i = 1, 2, \dots, \frac{n}{2} \quad (23)$$

$$x_i^{new} = x_{i-\frac{n}{2}} + rand \circ v'_i, \quad i = \frac{n}{2} + 1, \frac{n}{2} + 2, \dots, n \quad (24)$$

where  $x_i^{new}$  is the new position of the  $i$ th CB,  $rand$  is a random vector of size equivalent to the number of design variables, whose components are uniformly distributed within the interval of  $[-1, 1]$ , and the symbol " $\circ$ " refers to the element-wise product.

## 5. NUMERICAL EXAMPLES

In order to assess the effectiveness of seismic performance-based connection topology optimization approach, three optimization cases are taken into account as follows:

- 1)  $UF_S$ : Performance-based size optimization of unbraced steel frame with rigid beam-to-column connections.
- 2)  $UF_C$ : Performance-based connection topology optimization of unbraced steel frame.
- 3)  $XF_C$ : Performance-based connection topology optimization of X-braced steel frame.

Table 1: HSS cross-section database used for braces

HSS 2×2×0.125	HSS 4×4×0.500	HSS 6×6×0.375	HSS 8×8×0.375
HSS 2×2×0.250	HSS 4×4×0.187	HSS 6×6×0.500	HSS 8×8×0.500
HSS 2×2×0.187	HSS 4×4×0.312	HSS 6×6×0.625	HSS 8×8×0.625
HSS 3×3×0.125	HSS 5×5×0.125	HSS 6×6×0.187	HSS 8×8×0.187
HSS 3×3×0.250	HSS 5×5×0.250	HSS 6×6×0.312	HSS 10×10×0.250
HSS 3×3×0.375	HSS 5×5×0.375	HSS 7×7×0.250	HSS 10×10×0.375
HSS 3×3×0.187	HSS 5×5×0.500	HSS 7×7×0.375	HSS 10×10×0.500
HSS 3×3×0.312	HSS 5×5×0.187	HSS 7×7×0.500	HSS 10×10×0.625
HSS 4×4×0.125	HSS 5×5×0.312	HSS 7×7×0.625	HSS 10×10×0.187
HSS 4×4×0.250	HSS 6×6×0.125	HSS 7×7×0.312	HSS 10×10×0.312
HSS 4×4×0.375	HSS 6×6×0.250	HSS 8×8×0.250	

Table 2: Site class and spectral response acceleration parameters

Site class	Performance level	Hazard level	$S_{XS}$	$S_{X1}$
D	IO	20% per 50 year	0.835	0.396
	LS	10% per 50 year	0.937	0.455
	CP	2% per 50 year	1.196	0.588

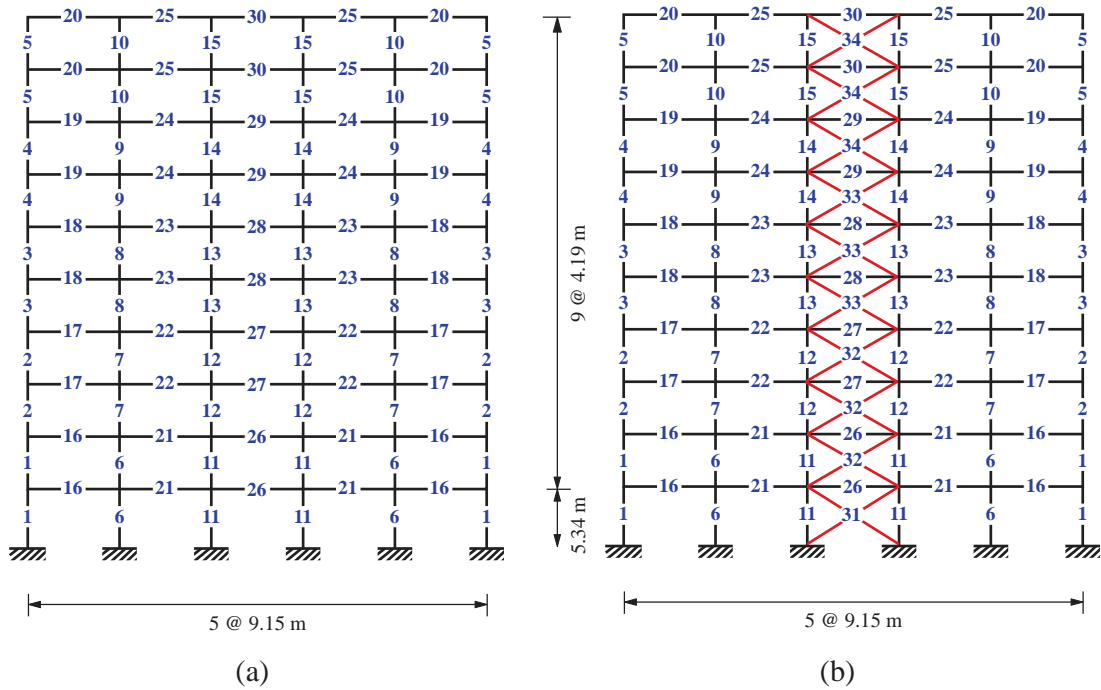


Figure 1. Design group numbers for: (a) unbraced steel frame and (b) X-braced steel frame

The general characteristics of the model such as geometry, material properties, dead loads, and live loads are assumed to be consistent with the five-bay, ten-story moment frame structure studied by Alberdi et al. [15]. An elastic perfectly-plastic behavior for the material is considered. In these examples, beams are selected from all 267 W-shaped sections and columns are chosen from W24, W21, W18, W16 and W14 sections. As described in [15], for the beams supported at their two ends by simple connections, the same cross-section (W14×22) is considered. The steel members utilized for braces in X-braced steel frame example are taken from a set of HSS sections tabulated in Table 1. The P-Δ effects are considered in the nonlinear pushover analysis. The site class and spectral response acceleration parameter values, which are reported in Table 2., are adopted in line with [8] and [9].

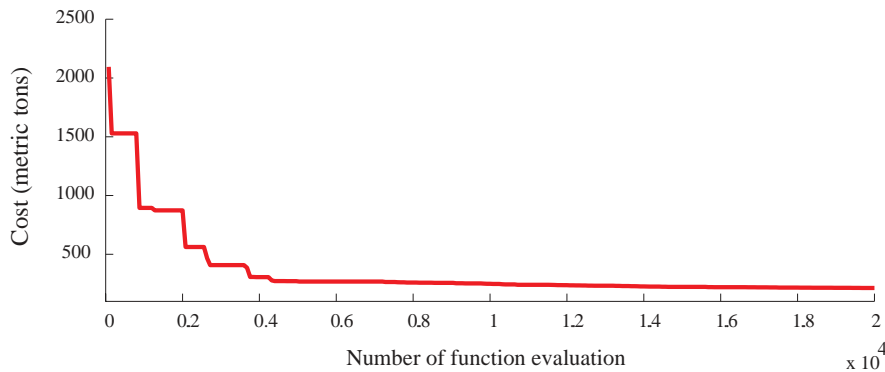


Figure 2. The convergence history curve for  $UF_5$

Table 3: Optimal designs for the three optimization cases

Member design group number	Frame ID		
	UF <sub>S</sub>	UF <sub>C</sub>	XF <sub>C</sub>
1	W24×84	W24×131	W21×44
2	W14×53	W18×40	W16×67
3	W14×90	W14×38	W24×68
4	W14×34	W14×43	W18×50
5	W21×73	W21×50	W14×53
6	W24×68	W18×211	W21×83
7	W18×106	W24×370	W24×84
8	W21×68	W24×146	W18×46
9	W24×68	W18×65	W24×55
10	W24×94	W24×56	W14×43
11	W24×68	W24×131	W24×306
12	W14×90	W21×111	W24×207
13	W14×90	W24×94	W21×147
14	W24×94	W24×229	W18×60
15	W21×55	W18×283	W18×71
16	W24×56	W24×84	W14×22
17	W18×45	W14×22	W14×22
18	W21×62	W14×22	W14×22
19	W12×22	W14×22	W14×22
20	W10×39	W14×22	W14×22
21	W24×55	W21×50	W14×22
22	W30×116	W30×134	W14×22
23	W21×57	W24×68	W14×22
24	W24×61	W14×22	W14×22
25	W12×26	W14×22	W14×22
26	W18×46	W14×22	W14×22
27	W12×19	W14×22	W14×22
28	W16×31	W14×22	W14×22
29	W18×46	W24×176	W14×22
30	W12×16	W14×22	W14×22
31	-	-	HSS 5×5×0.3125
32	-	-	HSS 10×10×0.25
33	-	-	HSS 7×7×0.375
34	-	-	HSS 6×6×0.187
Cost in metric tons	212.94	149.65	67.28

In this paper, OpenSees [26] is utilized to perform all required analyses. Also, the optimization algorithm is coded in MATLAB, and during the optimization procedure, MATLAB and OpenSees [26] are linked together. The programs are executed on a personal computer with Intel Core i7 CPU 4.0 GHz and 16GB of RAM. The population size is taken as 70 and 90 for the pure sizing and connection topology optimization, respectively. Moreover, the maximum number of function evaluations is set to 20,000 as the termination criterion for the CBO algorithm. In principle, each function of evaluation for the

optimization algorithm contains three structural analyses as: gravity analysis, elastic dynamic analysis, and nonlinear pushover analysis in accordance with what was described in previous sections.

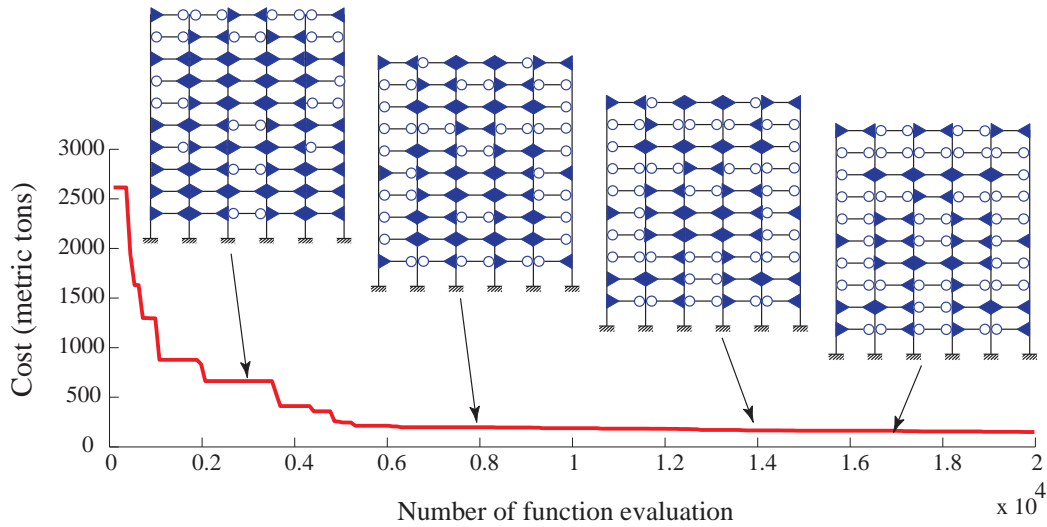


Figure 3. The convergence history curve for  $UF_C$

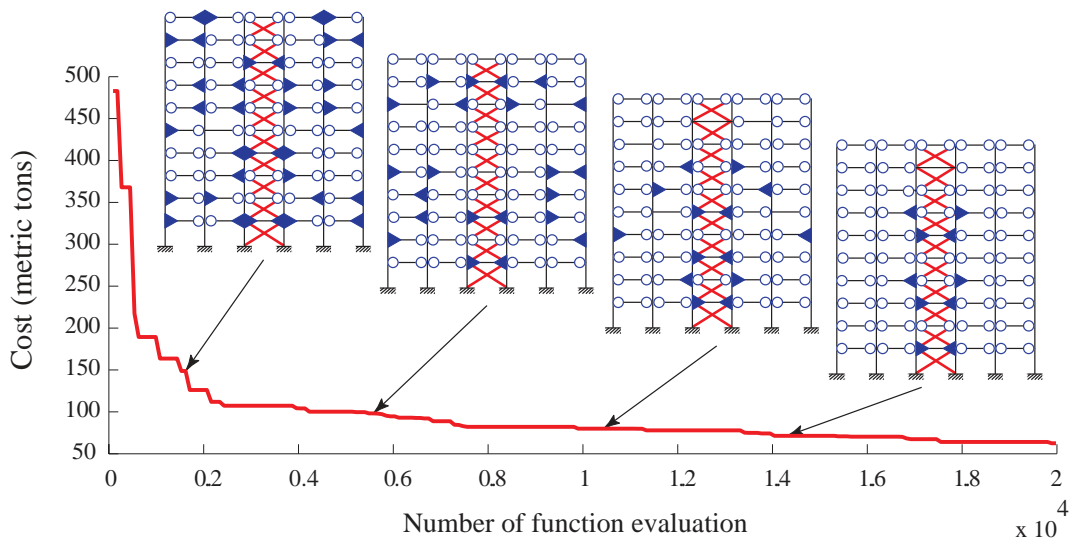
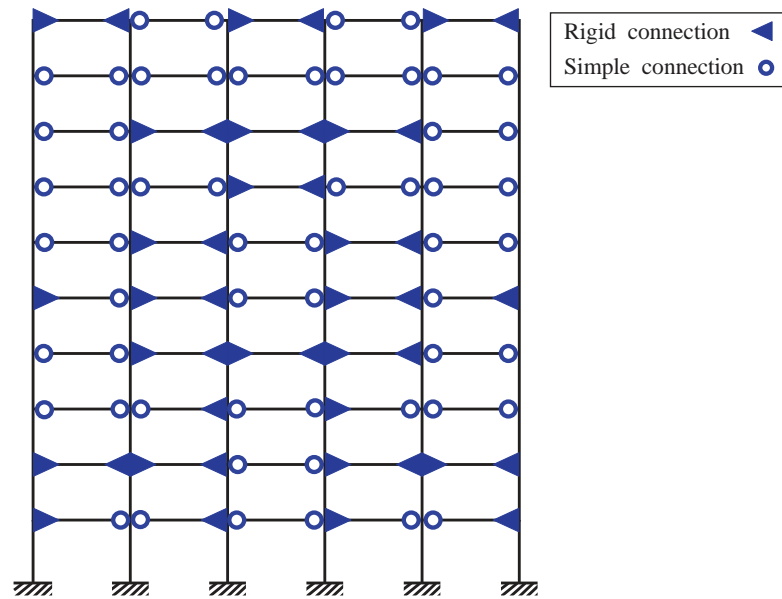
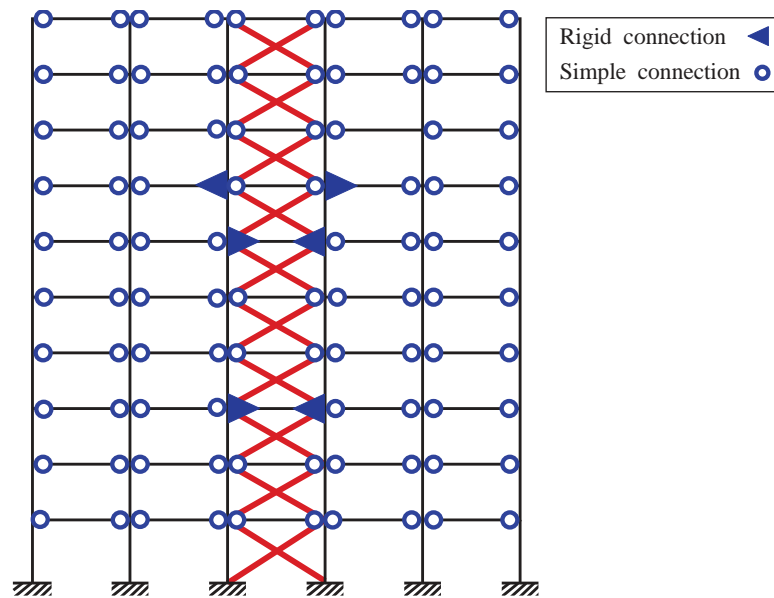


Figure 4. The convergence history curve for  $XF_C$

The basic models including assigned design group numbers for unbraced and X-braced steel frames are shown in Fig. 1.

The minimum total costs of the optimal designs generated by the CBO algorithm for the three optimization cases are reported in Table 3, which also presents the cross-sectional profile of their components. As shown, CBO algorithm achieved optimum designs with the equivalent weights of 212.94, 149.65, and 67.28 per metric tons for  $UF_S$ ,  $UF_C$ , and  $XF_C$ , respectively.

Figure 5. Optimal connection arrangement obtained for  $UF_C$ Figure 6. Optimal connection arrangement obtained for  $XF_C$ 

A comparison of the two results attained for  $UF_S$  and  $UF_C$  reveals that integrating the connection topology technique with performance-based seismic design concept can give rise to 30% reduction in the overall cost in comparison with performance-based pure sizing optimization. Furthermore, from the result gained for  $XF_C$ , it is evident that the total costs can be further reduced when performance-based connection topology optimization approach is applied to a X-braced frame.

The convergence history of the CBO algorithm for  $UF_S$ ,  $UF_C$ , and  $XF_C$  are presented in

Fig. 2, Fig. 3, and Fig. 4, respectively. The two last figures also illustrate how the structures evolve from their initial configuration to the configuration with better cost function value. It can be observed that the optimal degree of designs is strictly related to the number of rigid connections used for the frame. The arrangements of beam-to-column connections for the optimal solution of  $UF_C$  and  $XF_C$  are given in Fig. 5 and Fig. 6, respectively.

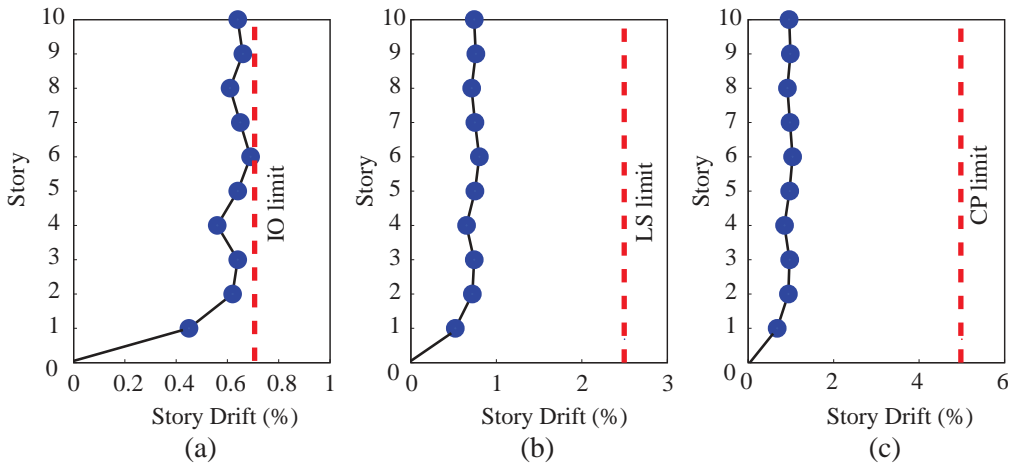


Figure 7. Inter-story drift ratios for  $UF_S$  at: (a) IO, (b) LS, and (c) CP performance levels

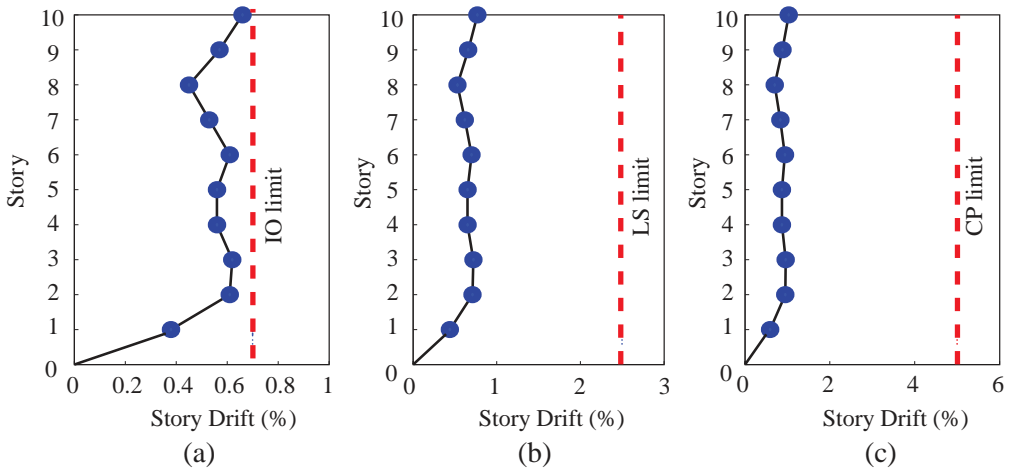


Figure 8. Inter-story drift ratios for  $UF_C$  at: (a) IO, (b) LS, and (c) CP performance levels

Inter-story drift ratios at various performance levels for  $UF_S$ ,  $UF_C$ , and  $XF_C$  are reported in Fig. 7, Fig. 8, and Fig. 9, respectively. As it is depicted, for all cases, inter-story drift constrain at IO level governs the design. The high economic design obtained for  $XF_C$  can be attributed to the high initial stiffness of the braced frame, which enables the structure to satisfy inter-story drift constraint associated with LS performance level in a more convenient way. Based on author's computations which is not reported here, if only LS and CP performance levels are considered for the optimization problem (i.e. IO level is discarded), the optimal costs of  $UF_C$  and  $XF_C$  become more close to each other.

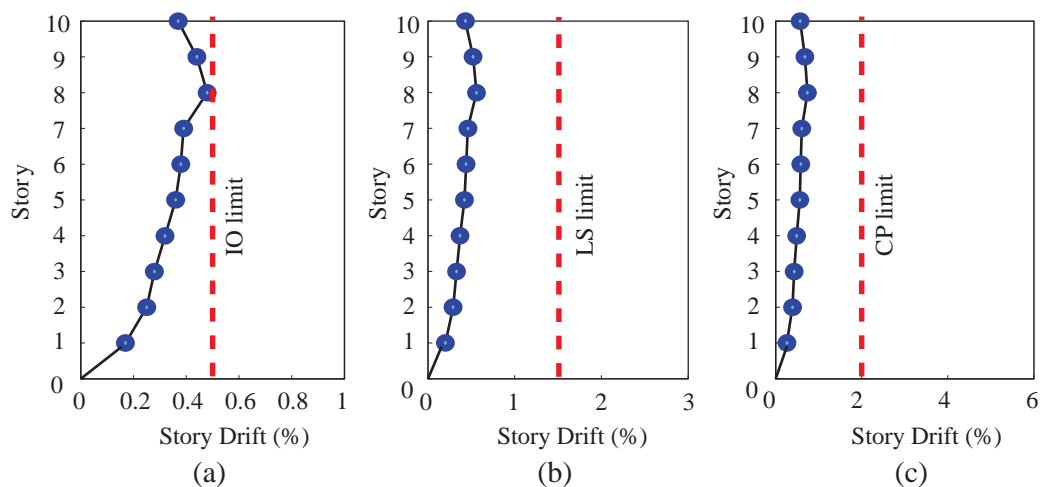


Figure 9. Inter-story drift ratios for  $XF_C$  at: (a) IO, (b) LS, and (c) CP performance levels

Fig. 10 compares the contributions of the structural components as well as rigid connections to the total cost of the optimized frames. As indicated, the economic efficiency of a design increases in accordance with a reduction in portion of rigid connection costs. Furthermore, it is apparent from the results that the optimal solutions obtained for  $UF_C$  and  $XF_C$  have a good tradeoff between the cost of their materials and connections.

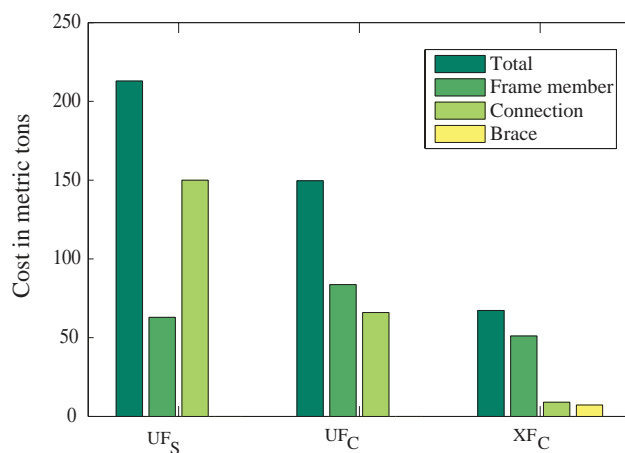


Figure 10. Comparison of material and connection costs for three optimization cases

## 6. CONCLUSIONS

This study aims to incorporate the performance-based seismic design approach into the connection topology optimization method with the intention of providing a new optimization concept. In this new concept, which called here performance-based connection topology optimization, the size of members and the type of connections are simultaneously optimized with regard to the framework of performance-based seismic design. In order to



evaluate the effectiveness of this new concept, it is applied to 5-bay, 10 story unbraced as well as X-braced steel frames. In this optimization problem, the cross-sectional area of components and the type of each beam-to-column connection (either simple or rigid) are considered as design variables. Moreover, the objective function is specified in terms of the material and rigid connection fabrication costs. The nonlinear pushover analysis is carried out to acquire the response of the structure at various performance levels. In order to handle the optimization task, CBO algorithm, which is a robust and parameter-less algorithm, is employed. Besides performance-based connection topology optimization, performance-based pure sizing optimization is also implemented for the numerical example as a basis for comparison. The achieved results indicate that when the optimal arrangement of the beam-to-column connections is participated in the optimum performance-based design process of either unbraced or X-braced steel frame, a much more cost-effective design can be generated. In addition, these findings provide further support for the connection topology optimization technique by expanding its application on the performance-based seismic design methodology.

## REFERENCES

1. Holland, J.H. *Adaptation in Nature and Artificial Systems*, The University of Michigan press, 1975.
2. Eberhart RC, Kennedy J. A new optimizer using particle swarm theory, *Proceedings of the Sixth International Symposium on Micro Machine and Human Science*, Nagoya, Japan, 1995, pp. 39-43
3. Dorigo M. *Optimization, learning and natural algorithms*, Ph. D. Thesis, Politecnico di Milano, Italy. 1992.
4. Hasançebi O, Çarbaş S, Doğan E, Erdal F, Saka MP. Comparison of non-deterministic search techniques in the optimum design of real size steel frames, *Comput Struct* 2010; **88**(17): 1033-48.
5. Doğan E, Saka MP. Optimum design of unbraced steel frames to LRFDAISC using particle swarm optimization, *Adv Eng Soft* 2012; **46**(1): 27-34.
6. Kaveh A, Talatahari S. Charged system search for optimal design of frame structures, *Appl Soft Comput* 2012; **12**(1): 382-93.
7. Kaveh A, Farhodi N. A unified approach to parameter selection in meta-heuristic algorithms for layout optimization, *J Construct Steel Res* 2011; **67**(10): 1453-62.
8. Kaveh A, Farhmand Azar B, Hadidi A, Sorochi FR, Talatahari S. Performance-based seismic design of steel frames using ant colony optimization, *J Construct Steel Res* 2010; **66**(4): 566-74.
9. Gholizadeh S, Moghadas RK. Performance-based optimum design of steel frames by an improved quantum particle swarm optimization, *Adv Struct Eng* 2014; **17**(2): 143-56.
10. Talatahari S, Hosseini A, Mirghaderi SR, Rezazadeh F. Optimum performance-based seismic design using a hybrid optimization algorithm, *Mathemat Probl Eng* 2014; **2014**.
11. Gholizadeh S, Poorhoseini H. Seismic layout optimization of steel braced frames by an improved dolphin echolocation algorithm, *Struct Multidisc Optim* 2016; **54**(4): 1011-29.

12. Hayalioglu MS, Degertekin SO. Minimum cost design of steel frames with semi-rigid connections and column bases via genetic optimization, *Comput struct* 2005; **83**(21): 1849-63.
13. Hadidi A, Rafiee A. A new hybrid algorithm for simultaneous size and semi-rigid connection type optimization of steel frames, *Int J Steel Struct* 2015; **15**(1): 89-102.
14. Kripakaran P, Hall B, Gupta A. A genetic algorithm for design of moment-resisting steel frames, *Struct Multidisc Optim* 2011; **44**(4): 559-74.
15. Alberdi R, Murren P, Khandelwal K. Connection topology optimization of steel moment frames using metaheuristic algorithms, *Eng Struct* 2015; **100**: 276-92.
16. Kaveh A, Ghafari MH, Gholipour Y. Optimum seismic design of steel frames considering the connection types, *J Construct Steel Res* 2017; **130**: 79-87.
17. Kaveh A, Mahdavi VR. Colliding bodies optimization: a novel meta-heuristic method, *Comput Struct* 2014; **139**: 18-27.
18. ASCE/SEI 41-06, *Seismic Rehabilitation of Existing Buildings*, American Society of Civil Engineers, Reston, Virginia, 2007.
19. Kaveh A, Laknejadi K, Alinejad B. Performance-based multi-objective optimization of large steel structures, *Acta Mech* 2012; **223**(2): 355-69.
20. Sahab MG, Toropov VV, Gandomi AH. A review on traditional and modern structural optimization: problems and techniques, *Metaheuris Applicat Struct Infrastruct* 2013: 25-47.
21. Kaveh A, Bakhshpoori T, Azimi M. Seismic optimal design of 3D steel frames using cuckoo search algorithm, *Struct Des Tall Special Build* 2015; **24**(3): 210-27.
22. ASCE/SEI 7-10, *Minimum Design Loads for Buildings and other Structures*, American Society of Civil Engineers, Reston, Virginia, 2010.
23. ANSI/AISC 360-10, *Specification for Structural Steel Buildings*, American Institute of Steel Construction, Chicago, Illinois, 2010.
24. Kaveh A, Mahdavi VR. Colliding bodies optimization method for optimum design of truss structures with continuous variables, *Adv Eng Softw* 2014; **70**: 1-12.
25. Kaveh A, Ilchi Ghazaan M. Optimal design of dome truss structures with dynamic frequency constraints, *Struct Multidisc Optim* 2016; **53**(3): 605-21.
26. Mazzoni S, McKenna F, Scott MH, Fenves GL. *OpenSees Command Language Manual*, Pacific Earthquake Engineering Research (PEER) Center, Berkeley, California, 2006.